Earth Evolution Sciences, Vol. 9, pp. 5-14, March, 1, 2015

Seismic activity and one-dimensional velocity structure along the Atotsugawa fault, from precise hypocenter relocations

Bogdan Enescu[a]*, Takuo Shibutani[b], Kiyoshi Ito[c], Shiro Ohmi[b], Hiroo Wada** [b]

[a]*Graduate School of Life and Environmental Sciences, University of Tsukuba, Ibaraki 305-8572, Japan*
[b]*Disaster Prevention Research Institute, Kyoto University, Gokasho, Uji, Kyoto 611-0011, Japan*
[c]*Center for Integrated Research and Education of Natural Hazards, Shizuoka University, Otani 836, Suruga, Shizuoka 422-8529, Japan*

**E-mail: benescu@geol.tsukuba.ac.jp ; **Retired*

Abstract

Using *P*- and *S*- wave arrival time data and the initial hypocenter locations of the Disaster Prevention Research Institute (DPRI), Kyoto University, we relocate the earthquakes that occurred from 1997 to 2005 in the Atotsugawa fault region, central Honshu, Japan. We use all the events of magnitudes $M \geq 0.0$, which have at least six P-wave phase picks and at least one *S*-wave phase pick. We first apply a Joint Hypocenter Determination (JHD) technique on a subset of earthquakes with $M \geq 1.0$ to determine a better 1D velocity model for the region and station corrections for the *P* and *S*-wave arrivals. The obtained travel time residuals agree well with the shallow geologic structure; relatively large positive station corrections are obtained for the thick sedimentary structure of the Toyama basin, located at north and north-east from the fault system, while negative residuals characterize the fault area, known for the old Hida metamorphic rocks. Using the new 1D velocity model and station corrections we do a single-event location for all our earthquake data to obtain the best absolute hypocenter locations. We further improve the hypocenter location of earthquakes using a double-difference (DD) approach. The variance reduction after the single-event locations is 73%, while the DD relocation reduces further the variance by 70%. The epicentral map of the DD-relocated earthquakes shows clear lineations and clustering. The seismicity in NW-SE cross-sections, perpendicular to the earthquake lineations, defines clear clusters of events that correlate well and thus confirm the geologically known Ushikubi, Mozumi and Atotsugawa faults. The clear separation of the nearby Mozumi and Atotsugawa active faults is one of the main new findings of this study. A SW-NE cross-section through the hypocentral distribution, along the fault system, shows a central area with fewer earthquakes, which is known for its relative quiescence and correlates well with detected aseismic creep from geodetic measurements.

Keywords: Atotsugawa fault system, seismicity, geologic structure, precise earthquake locations

Introduction

The Atotsugawa fault system is one of the prominent active fault systems in central Honshu, Japan (Matsuda, 1966). It consists of three main strike-slip faults, the Atotsugawa, Ushikubi and Mozumi-Sukenobu faults, with a total length of about 80 km, striking east-north-east. An *M*7.0 earthquake occurred here in 1858 and caused severe damage in the region. The fault slip rate for the past one million years along the Atotsugawa fault exceeds 1.5 mm/y, which falls in the group of a highest fault slip rate in Japan (The Research Group for Active Faults, 1991). The Atotsugawa fault system is located in the central part of the so-called Niigata-Kobe Tectonic Zone (NKTZ), which is recognized as a region of large strain rates, distributed along the Japan Sea coast and in the northern Chubu and Kinki district, from the analysis of GPS array data (Sagiya et al., 2000). The high horizontal strain rates in the NKTZ region have been discussed in terms of an interplate deformation (e.g., Shimazaki and Zhao, 2000) or intraplate deformation (e.g., Iio et al., 2002). Nakajima and Hasegawa (2007) revealed the existence of a low-velocity zone in the lower crust along the NKTZ and suggested that the inelastic deformation in the lower-crust contributes to the large contraction at the surface.

The seismicity in the region has been monitored by a seismological network since 1977. The seismic signal was initially telemetered from stations to Kamitakara observatory (DPRI, Kyoto University). From 1996, the telemeter system was completely replaced by a satellite communication system and the data recording/processing was improved. The station numbers recorded at the Kamitakara observatory increased to more than 50 with a high dynamic range of 22-24 bits/data unit (Ito and Wada, 2002).

Earthquakes in the Atotsugawa fault system are relatively small and the maximum magnitude is 4.6 during 1977-2005. However, most of events with $M1.5$ or larger can be detected by the network in all the observation period (Wada and Ito, 1995; Ito et al., 2007a). Although the earthquake distribution shows NE-SW linear trends parallel to the fault traces, a spatial heterogeneity of the seismicity along the Atotsugawa fault system has been also recognized (Mikumo et al., 1988; Ito and Wada, 2002; Ito et al., 2007a, b). Thus, the seismicity in the central part of the Atotsugawa fault is rather low compared with that in the eastern and western parts of the fault. Geodetic measurements of baseline length by an optical distance-meter across the Atotsugawa fault (Geospecial Information Authority of Japan (GSI), 1997) revealed creep-like movements at a rate of about 1.5 mm/year within the central segment of the fault; however no baseline change has been observed on the western segment of the fault.

The main goal of the present study is to obtain improved hypocenter locations in the Atotsugawa area, using the arrival-time data of earthquakes recorded from 1997 to 2005 at Kamitakara observatory. We also derive a 1D velocity model, which could be used as a starting model in tomographic studies and station corrections that give some insight on the local, shallow geologic structure.

The careful relocation of events using both a Joint Hypocenter Determination (JHD) method (Kissling et al., 1994) and a double-difference (DD) technique (Waldhauser and Ellsworth, 2000) allow characterizing in detail the spatial distribution of seismicity within

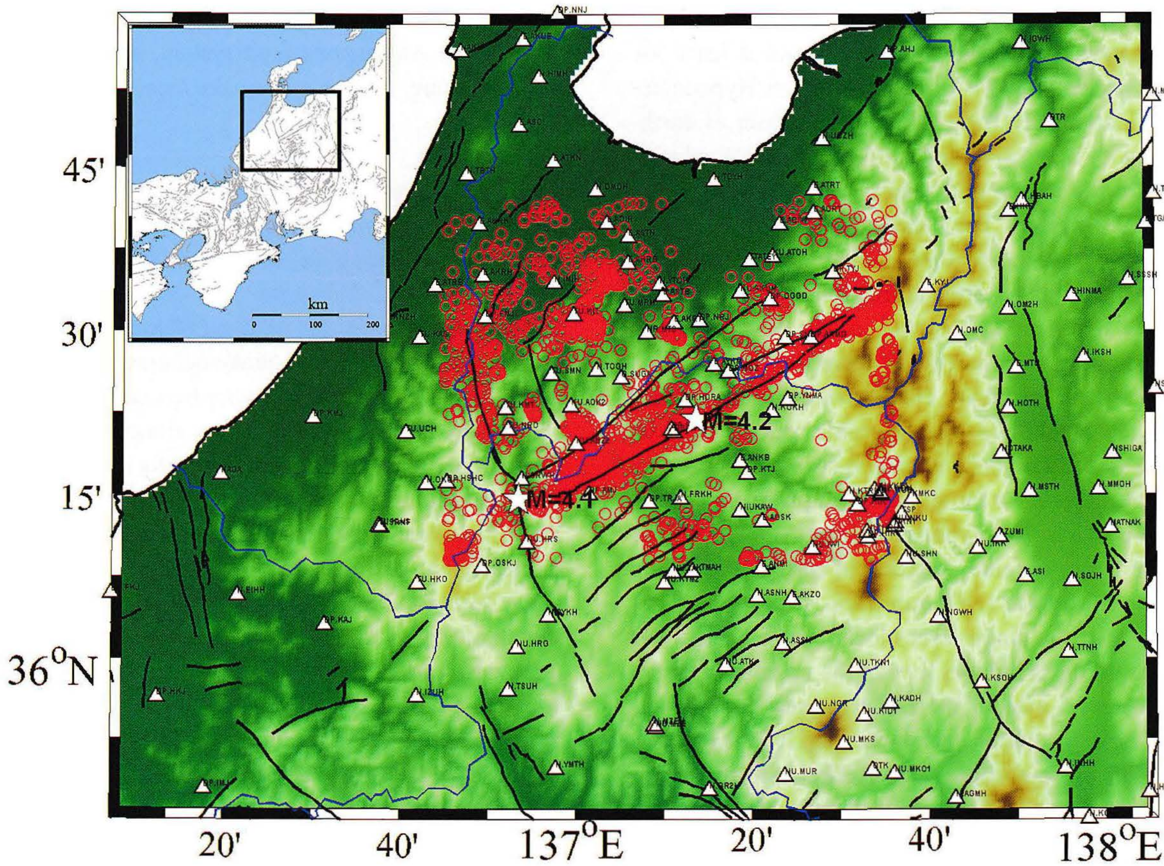

Fig. 1 Distribution of initial epicenters (DPRI catalogue data, 1997 – 2005, 3148 events) and seismic stations used in this study. The events were selected based on the following criteria: $M \geq 0.0$; no. of P-wave phase picks ≥ 6 and no. of S-wave phase picks ≥ 1. Earthquakes and stations are represented by red circles and white triangles, respectively. Largest events are marked by stars. The inset shows as a rectangle the location of the study area in Central Japan.

and close to the fault regions. In the last part of the paper, we compare the initial locations with the different relocations results in an attempt to better understand the advantages of each relocation technique.

Data and method of analysis

The data used in this study consist in *P*- and *S*-wave arrival times of earthquakes recorded at Kamitakara observatory from 1997 to 2005, which occurred in an epicentral area defined by 36° 9' – 36° 42' N latitude and 136° 42' – 137° 39' E longitude (Fig. 1). There are 3148 events in total. In this work we used 144 seismic stations, which are located in a larger region, as can be seen in Fig. 1. The arrival times used in this study were picked manually by one researcher, so the reliability and accuracy of the picks is high. Some of the earthquakes occurred from November 2004 to June 2005 were located using the arrival times at the permanent stations, as well as at a few temporary stations operated by the Earthquake Research Institute (ERI), University of Tokyo, and deployed for intense observations in the region by the "Japanese University Group of Joint Seismic Observations at NKTZ" (The Japanese University Group of the Joint Seismic Observations at NKTZ, 2005). The analysis procedure starts with the determination of an improved 1D velocity model and station corrections, using a JHD technique. In this way, one could obtain more accurate absolute hypocenter locations. The refinement of earthquake locations is done using a double-difference approach, which improves the relative hypocenter locations. The relocation of earthquakes is done in three steps:

Method of analysis - Step 1

We selected 917 events with the following criteria: (1) the number of *P*- arrival times was greater than five; (2) the number of S- arrival times was at least one; (3) the magnitude of the events was $M \geq 1.0$. We determined simultaneously the hypocentral parameters, 1D velocity models of *P*- and *S*- waves and the travel time corrections of *P*- and *S*- waves for all the stations using a JHD technique (Kissling et al., 1994). The accuracy of the *P*- and *S*-picks for the selected earthquakes (using the above criteria) is less than 0.08 s and 0.2 s, respectively. In the inversion the weight of the *S*-waves was chosen as 50% of that of the *P*-waves.

We carried out two iterations with different damping factors, following a similar procedure with Shibutani et al. (2005). For the first iteration, the damping parameters were set to 0.01 for the hypocentral parameters, 1.0 for the velocity parameter and 0.1 for the station corrections. For the second iteration, the same parameters were set to 1.0, 0.001 and 1.0, respectively. Practically, the location of the hypocentres and the station corrections are determined during the first iteration, while the velocity model is determined during the second one. By doing so, we also obtain an average of the station corrections close to zero.

Method of analysis - Step 2

In the second step of the analysis we performed single-event relocations for all the events which satisfy the criteria (1) and (2) and have magnitudes larger than zero. We use the velocity structure and station corrections previously determined and the damping factors for the hypocentral parameters were set to the same values as for the first iteration of the JHD relocation. In this way, we obtain the best absolute locations given the 1D velocity structure obtained from JHD.

Method of analysis - Step 3

To further improve the relative location of the events, in particular of those that are in the proximity of the faults, we use a program to compute double-difference hypocenter locations (hypoDD) (Waldhauser and Ellsworth, 2000). The method minimizes the residuals between observed and theoretical travel-time differences (or double-differences) for pairs of earthquakes at each seismic station while linking together all observed event-station pairs. A least-square solution is found by iteratively adjusting the vector difference between the hypocentral pairs. We use the 1D velocity model obtained from the JHD, at *Step 1*. We performed nine iterations to obtain the final solution. For all iterations the weight of the *S*-waves was 50% of that of the *P*-waves. For the first three iterations we used a relatively high damping factor and no constrains for the travel-time residuals and distance between the earthquake in a pair. For the following six iterations we chose gradually smaller residual thresholds and damping factors and we also limited the maximum distance allowed for earthquakes to form a pair. The number of earthquakes after relocation is 2978.

Results and Discussion

We present in Fig. 2a the initial and the JHD-determined 1D velocity models for Atotsugawa area. There are a few differences between the two models, notably concerning the *P*-wave velocity. The JHD-determined *P*-wave velocity is larger than the *P*-wave velocity used at the Kamitakara Observatory in the upper few kilometres of the model and becomes slightly smaller than the initial *P*-wave velocity below ~4km. Note that the *P*- and *S*-wave velocities are very well resolved down

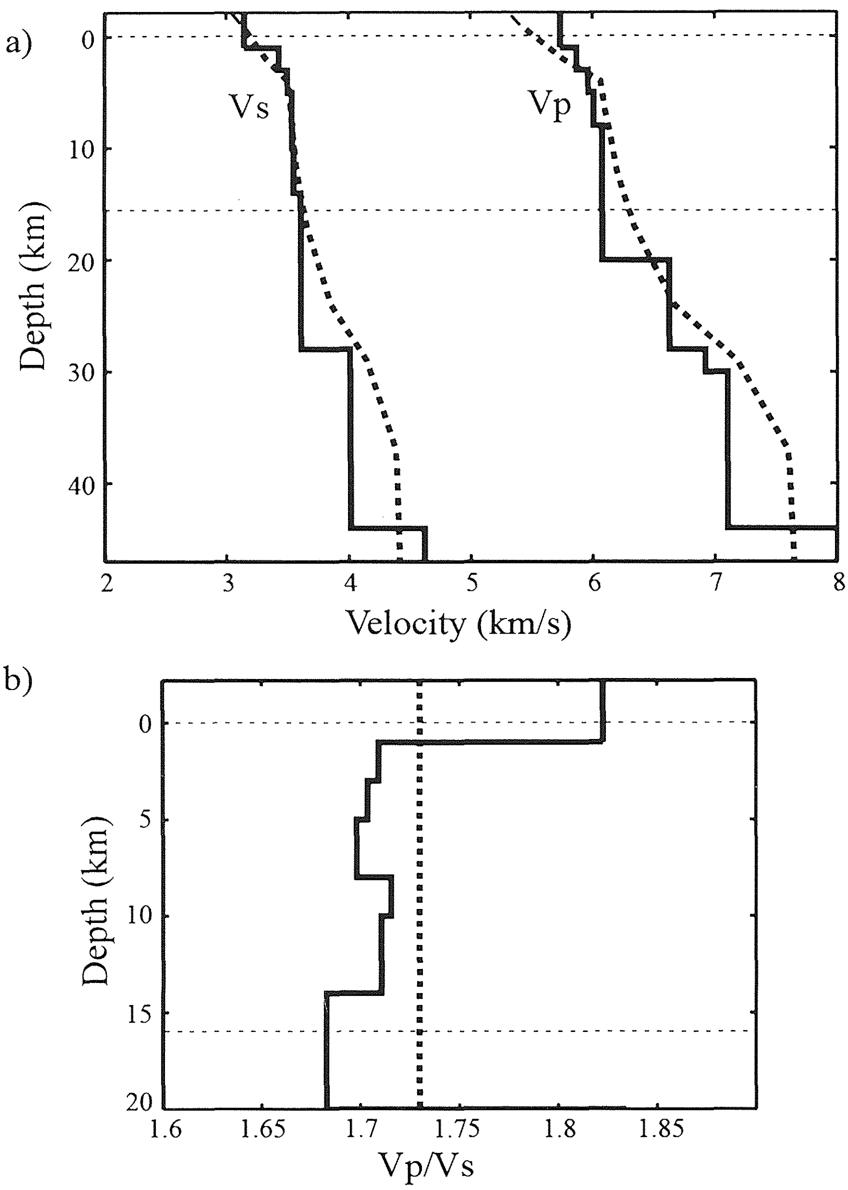

Fig. 2 a) 1D velocity models for the *P*- and *S*- waves (in km/s). b) *Vp*/*Vs* ratio. The dotted and continuous lines indicate the model used at Kamitakara observatory and that obtained from the JHD relocation, respectively; Horizontal lines indicate the depth limits where JHD results show high resolution to determine *Vp* and *Vs* accurately.

to a depth of about 16 km, since the ray hit parameter, which quantifies the ray coverage at a certain place, is relatively large (greater than 800) above this depth. The standard errors for both the *Vp* and *Vs* are smaller than 0.05 km/s at most depths levels. The variation of *Vp* and *Vs* versus depth obtained here should reflect an average structure over the study area. However, since most of the earthquakes and stations are situated within or close to the fault region, the obtained *Vp*, *Vs*, and *Vp*/*Vs* in the shallow part of the model are probably representative for this area, with the highest density of rays. Seismic surveys conducted in the fault region (Ueno et al., 2005; Ito et al., 2007b) indicate shallow *Vp* velocities that are faster than those used for routine hypocenter determination at Kamitakara Observatory. Our results are consistent with these observations. The JHD-determined *Vp* and *Vs* values are also generally consistent with those obtained by Kato et al. (2006, 2007) from a local tomography study in the Atotsugawa region.

Fig. 2b shows the variation of the *Vp*/*Vs* ratio as a function of depth. The ratio has a relatively large value (~1.8) in the very shallow part of the crust and drops to moderate values (~1.7) at depth. Kato et al. (2006, 2007), in their tomographic studies, report a similar decreasing trend for the *Vp*/*Vs* ratio.

Figure 3 shows in a map view the station corrections, in seconds, for the *P*-wave. The station corrections ac-

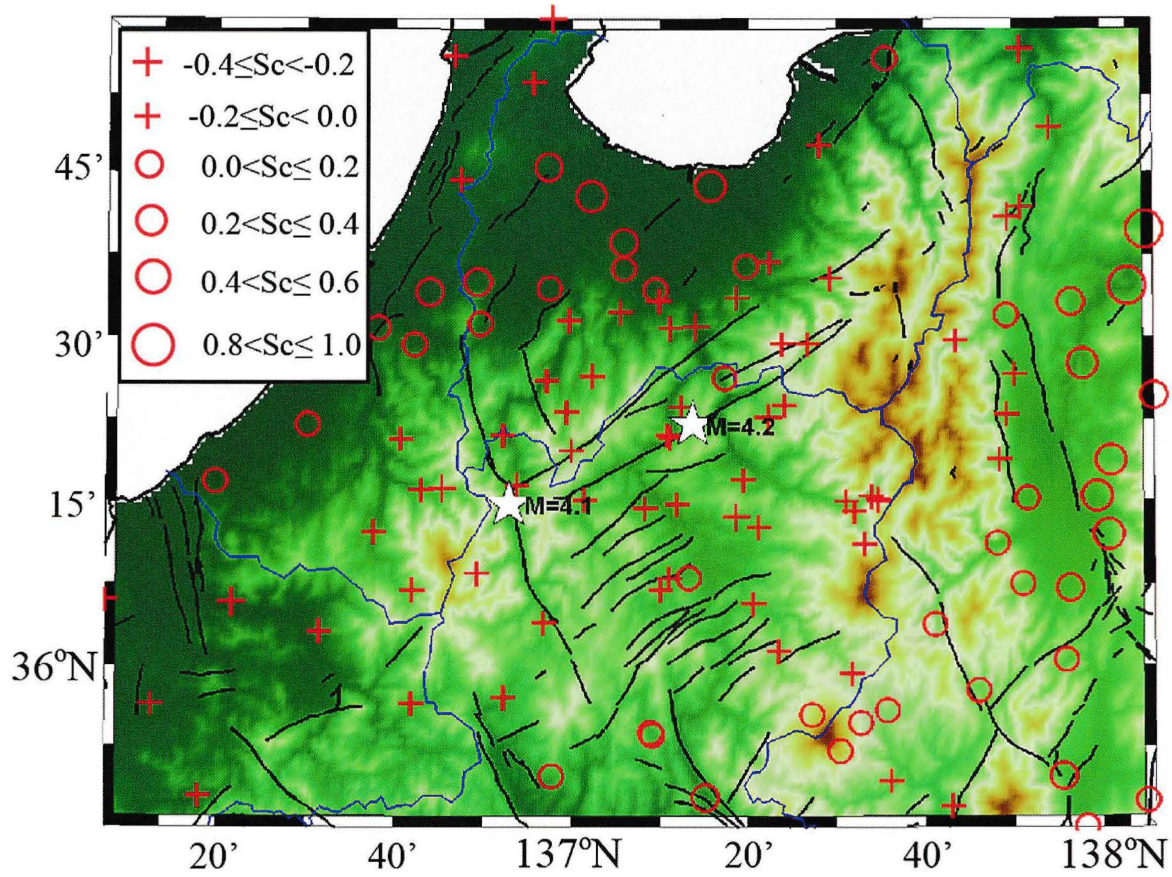

Fig. 3 Station corrections (in seconds) for the *P*-wave, as obtained using the JHD approach. The red circles and crosses indicate the positive and negative residuals, respectively. Reference sizes are shown in the inset.

count for the three-dimensionality of the velocity field that cannot be adequately represented by a 1D velocity model (Kissling et al, 1994). They are strongly coupled to the velocity structure just beneath the station (Kissling et al., 1994; Shibutani et al., 2005). In our analysis as well, the sign and amplitude of station corrections reflect, in general, the characteristics of the shallow geologic structure (Geological Survey of Japan (GSJ), 2002). Large positive travel time residuals can be found in the north and north-east parts of the study region, in the Toyama Basin, known for the thick sedimentary cover. The eastern side of the map in Fig. 3 shows also relatively large, positive, station corrections. They correspond to the Matsumoto basin, with Quaternary sedimentary cover. The areas of relatively high-seismicity of the Atotsugawa fault system (central part of the map) are mostly characterized by relatively small negative residuals, which probably reflect the harder, metamorphic rocks present in the region. It can be also noticed, however, that at one particular site situated within the fault region, the station correction is negative. This may reflect the fact that the creeping section of the fault (see below for discussions) is characterized by lower velocities, compared with the neighbouring regions (Kato et al., 2007; Nakajima et al., 2010). A similar station correction pattern was obtained for the *S*-wave. We have checked the stability of our 1D velocity model and station corrections, by applying the JHD technique to different subsets of data: in all cases there are no significant differences between the results.

Figure 4 shows the epicentral distribution of earthquakes after single-event relocation (i.e., after *Step 2* - see previous section), using the 1D velocity model and station locations determined at *Step 1*. We plot only the best relocated events in terms of epicentral and depth errors (i.e., earthquake locations with epicentral and depth errors less than 0.2 km and 0.5 km, respectively). It can be noticed that the epicentres in the central part of the map define clear SW-NE trends, following in general the traces of the three main faults that define the Atotsugawa system: the Ushikubi fault, the Mozumi-Sukenobu fault and the Atotsugawa fault. In other places, to the north and south of these three main faults, the

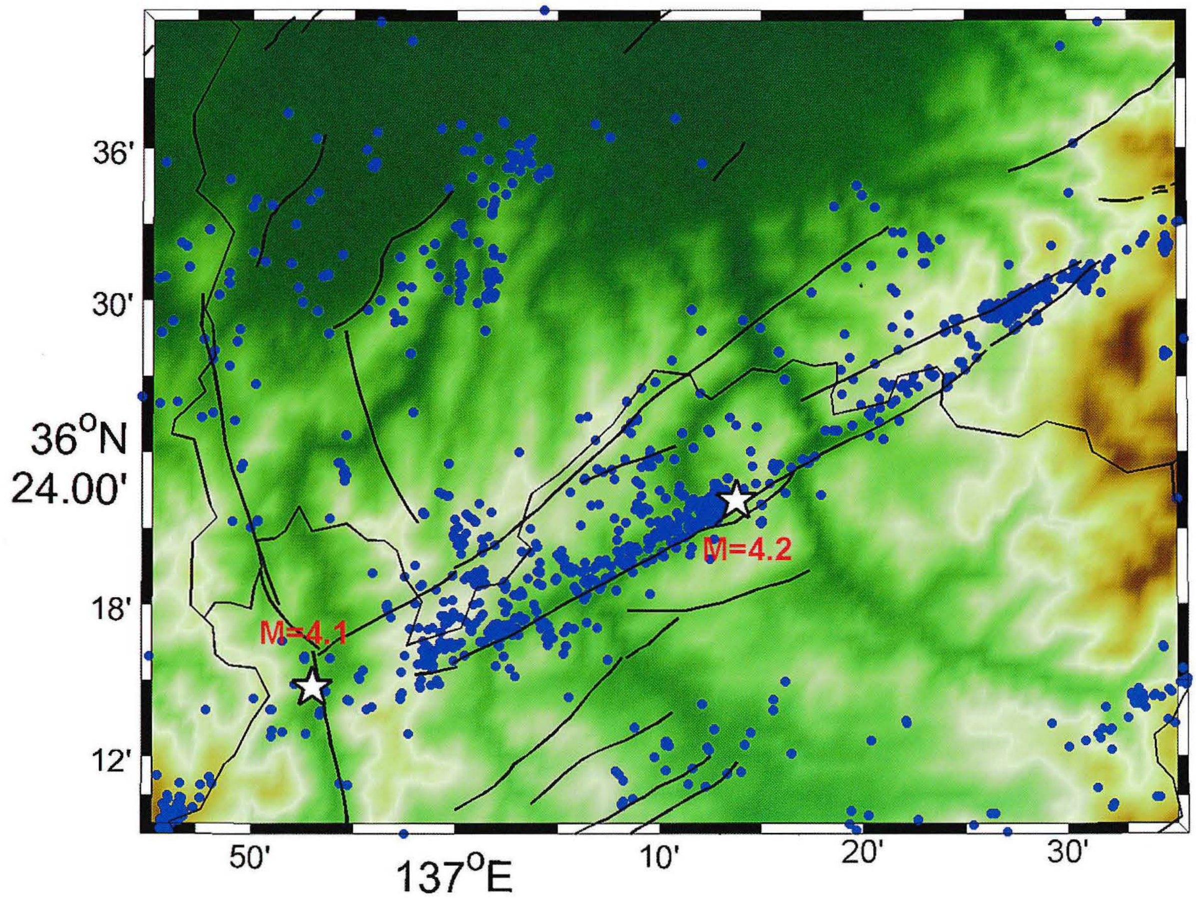

Fig. 4 Epicentral distribution of earthquakes after JHD and single-event relocation. Only events that have the epicentral error smaller than 0.2 km and the depth error smaller than 0.5 km are plotted.

number of events is rather small for some conclusive results. However, although there is considerable scatter, it can be noticed that also for these off-central areas there is some agreement between the distribution of seismicity and the location of geologically known fault structures. We will explore further the distribution of seismicity after double-difference relocation (i.e., after *Step 3*), in the areas where the number of earthquakes is significant enough for a detailed characterization.

Figures 5a), b) and c) show the epicentral maps for the original locations and for the relocations performed at Steps 2 and 3, respectively. The red arrows in each of these maps indicate a segment of the Mozumi-Sukenobu fault, along which the epicentral distribution of earthquakes shows a clearer linear trend after relocation. An even sharper image can be seen close to the NE end of the fault system (see the blue arrows in the figures), where the epicenters along the Mozumi-Sukenobu fault show a clear lineation along the fault trace after the single-event relocation, using station corrections; the linear distribution of epicenters becomes even sharper after double-difference relocation.

The hypocenter distribution in a cross-section from A to B (see the epicentral maps) reveals important differences between the original depth locations (Fig. 5d) and the relocation results (Figs. 5e, f). Thus, the relocation of earthquakes using station corrections and the new 1D velocity model shifts some earthquakes to very shallow depths in the SW part of the fault system (Fig. 5e). On the other hand, at the NE end of the profile, the earthquakes become deeper (Fig. 5e), compared to the initial hypocenters (Fig. 5d). The depth of the lower cut-off of seismicity along the profile shows a smaller variation after the single-event relocation. Note that the number of earthquakes after single-event locations is the same as that in the original catalogue (i.e., 3148 events). The further application of the DD method shifts some of the very shallow events above surface (i.e., above 0 km depth), so the total number of relocated events decreases with 170. While the differences discussed above are rather small, they are larger than the hypocenter uncertainties and therefore significant. Dense earthquake observations in the area, like those done by the "Japanese University Group of Joint Seis-

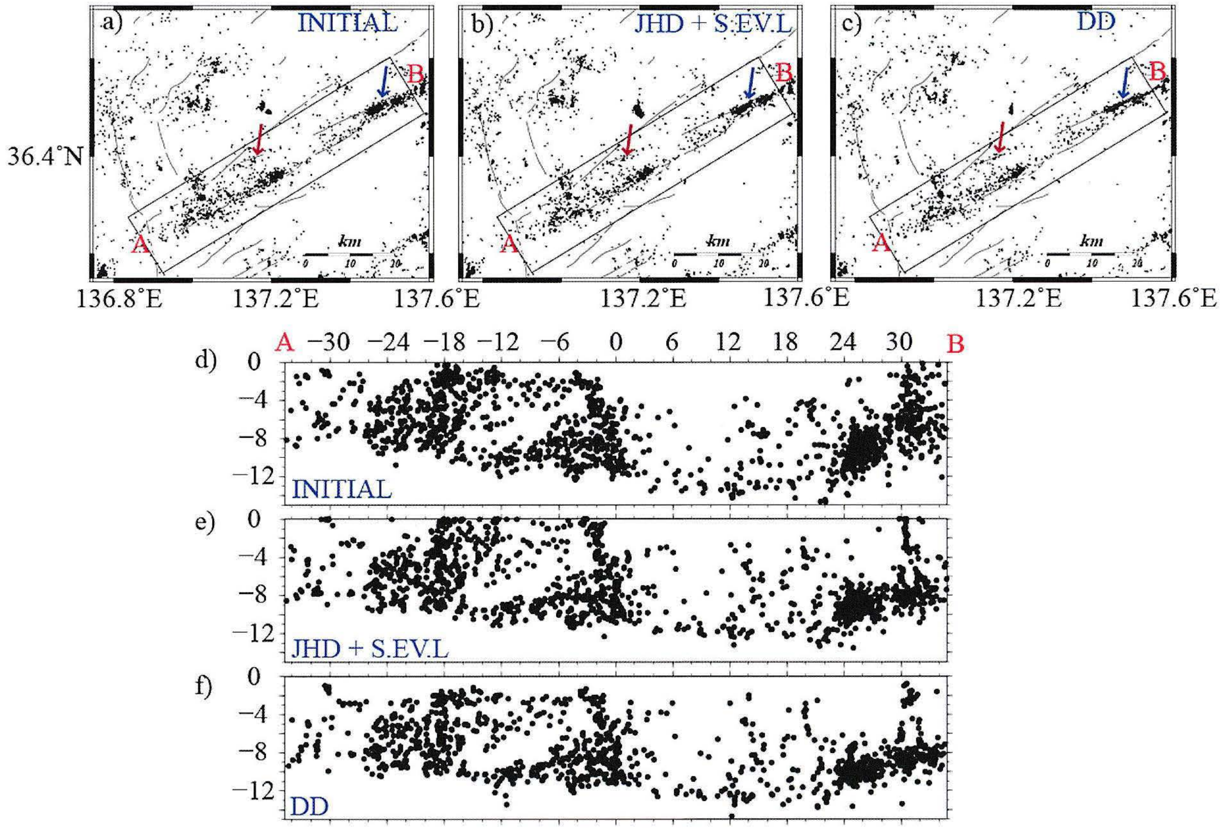

Fig. 5 Epicentre maps of the a) initial earthquake locations; b) single-event relocations using station corrections and the 1D velocity model determined by applying the JHD method; c) DD relocations of earthquakes. d), e) and f) show projected hypocenter locations along a profile oriented from A to B in a), b) and c), respectively. All earthquakes with epicenters within the rectangle area defined in the maps are used for the projection. The red and blue arrows in the epicentral maps indicate along-fault regions were the relocations show sharper epicentral distributions (see text for discussion).

mic Observation at NKTZ", will make possible to invert for the detailed 3D velocity structure, as well as for the location of earthquakes and elucidate the relation between the crustal structure and the distribution of earthquakes in the Atotsugawa fault region. Such more refined analyses, based on newer and updated data, will be considered for future studies.

Figure 6a shows the epicentral map of earthquakes along the Atotsugawa fault system, after the DD relocation. There are in total 2978 relocated events, with an average RMS residual of 2.5 ms. We focus on the areas along the Mozumi-Sukenobu and Atotsugawa faults, where the relocated seismicity is more abundant. One can notice sharp distributions of events, subparallel to the traces of both Mozumi and Atotsugawa faults.

We present in Fig. 6b a cross-section from A to B (see Fig. 6a for the location of the profile) perpendicular to the two faults. One can notice the clear separation of two earthquake clusters, dipping almost vertically, corresponding to the Mozumi fault and Atotsugawa fault, respectively. The separation of the clusters is especially clear at depths below 5 km. Figure 6c shows a cross-section from C to D (see Fig. 6a), in the NE side of the fault system. While the separation is less clear in this cross-section, one could still identify two main earthquake clusters below about 6 km depth. It is likely that the two clusters belong to the Mozumi and Atotsugawa fault, respectively. It is difficult, however, to explain how the two faults extend to the surface since the seismicity shallower than 5-6 km does not show any clear structure. Moreover, the event locations in the shallower part are less accurate, so we cannot establish whether the faults intersect there. If we assume that the faults are quasi-vertical, which appears to be the case in Fig. 6b, we could infer that the Mozumi fault, defined by the NW cluster, has mainly deeper earthquake activity (between 6 and 12 km), while the earthquakes on Atotsugawa fault extend from around 1 to 12 km.

Figure 6d shows in a cross-section from SE to NW the distribution of seismicity along the entire fault system. The earthquakes are deeper in the central part and become shallower to the NE and SW. Between about 50 and 77 km along the cross-section, there is an area of low-seismicity, which is flanked by high-seismicity

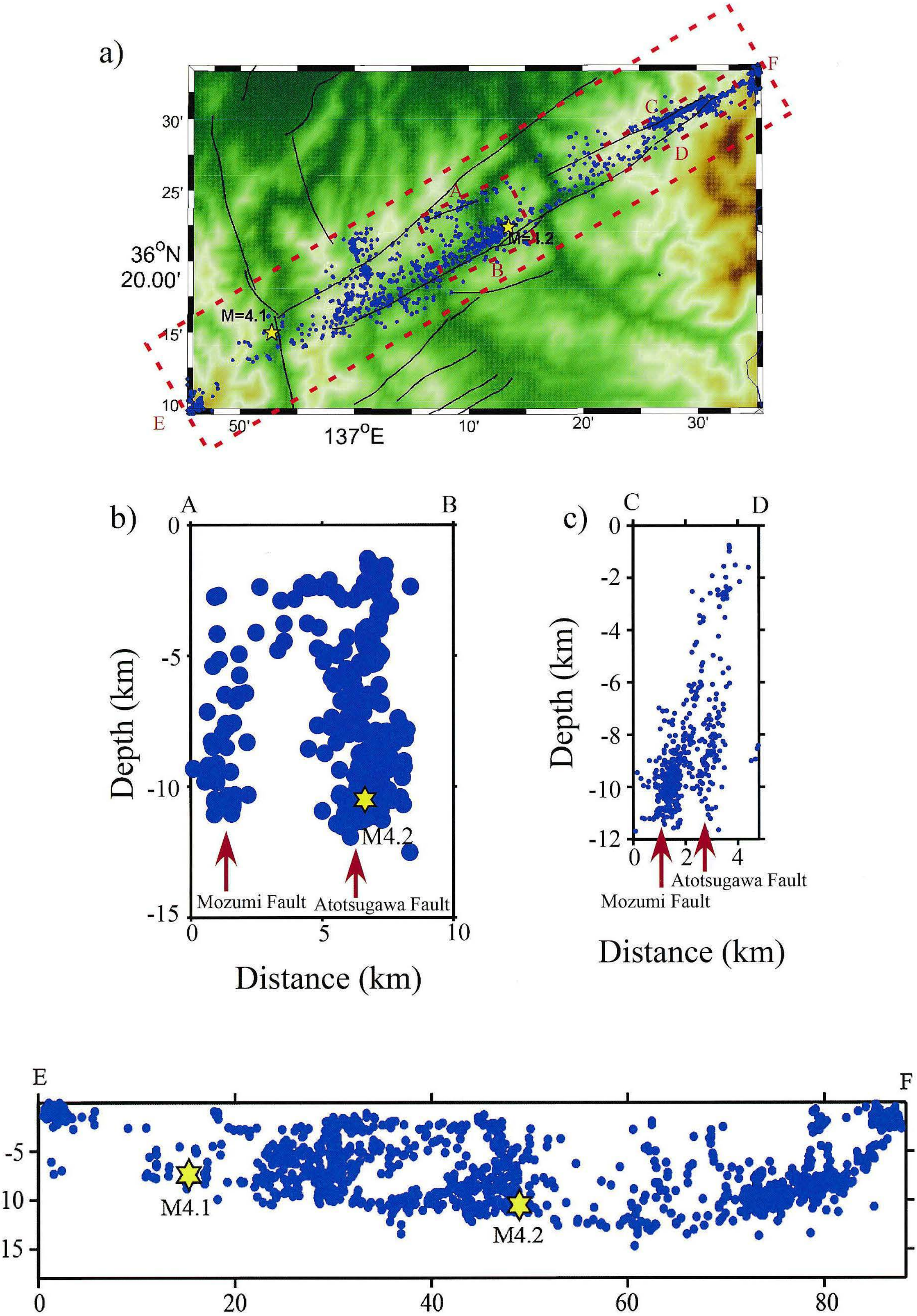

Fig. 6 Double-difference relocation results: a) Epicentral distribution of earthquakes after relocation. A-B, C-D and E-F indicate profiles used for the cross-sections. The dotted rectangles delimit the earthquakes that were used in each cross-section. b) A to B cross-section; c) C to D cross-section; d) E to F cross-section.

areas. This area of low-seismicity corresponds to a region of creep-like movements, as pointed out in previous studies (e.g., Ito et al., 2007a). Earthquakes in the creeping section are the deepest along the entire Atotsugawa fault. A striking feature of this cross-section is the sharp cut-off depth of seismicity. The largest earthquakes during the observation period (two events of *M*4.1 and *M*4.2) occurred at the base of the seimogenic layer. As pointed out in previous studies, the depth of the seismogenic layer is well correlated with the surface heat flow or the thermal structure of the crust (Sibson, 1982; Ito, 1990). Since there are active volcanoes at both ends of the Atotsugawa fault, the decrease in the cut-off depth towards both ends of the fault can be explained by a change in the thermal structure (Sibson, 1982). The deeper seismicity in the creeping section of the fault could be related with a larger slip rate at depth (Sibson, 1982; Ito et al., 2007a).

Conclusions

We have used the earthquake data recorded at Kamitakara Observatory, Kyoto University, from 1997 to 2005, to obtain an improved 1D velocity model, station corrections and accurate hypocenter locations in the Atotsugawa fault region. We first use the JHD method with a subset of earthquake data to obtain a better 1D velocity model and station corrections. Then, we use a single-event location method to relocate all the earthquakes. In this way we obtain accurate absolute hypocenter locations. To explore in more detail the seismicity along the Atotsugawa fault system, we further use the double-difference approach to get better relative earthquake locations.

The 1D velocity structure obtained after JHD shows some differences compared to the initial model used at Kamitakara observatory. For the *P*-wave in particular, the new velocity model has larger values at surface and slightly smaller at depth, compared to the initial model. The *Vp*/*Vs* ratio has relatively large values at very shallow depth and becomes small to moderate in the deeper part. The station corrections are consistent in general with the shallow geologic structure. Relatively large positive values are found in areas with thick sediment (Toyama and Matsumoto basins) and negative values are found around Atotsugawa fault system, in a region of old metamorphic rocks.

The distribution of relocated earthquake epicenters shows sharp linear trends, oriented from SW to NE, subparallel to the Ushikubi, Mozumi-Sukenobu and Atotsugawa fault traces. Cross-sections along profiles perpendicular to the fault traces reveal a clear clustering of hypocenters: the earthquakes that occur along Mozumi and Atotsugawa faults are clearly separated especially at depths greater than about 5-6 km. This is one of the most important new findings of this study; note that such clear separation of nearby active faults might be difficult to observe in Japan, where the preponderance of a compressional regime leads to the formation of many thrust-type faults characterized by more complex spatial seismicity patterns (Shibutani et al., 2005). A cross-section along the Atotsugawa fault system shows a relatively sharp lower cut-off depth of seismicity; the earthquakes along the fault are shallower at both south-west and north-east ends of the fault and become gradually deeper in the central and north-eastern segment, where an area of low seismic activity is apparent.

The depth of the relocated hypocenters shows some differences compared to the initial ones. Thus, after single-event relocation using station corrections, some of the hypocenters in the SW part of the fault system are getting very shallow, while in the NE end of the fault system the shallow hypocenters are becoming deeper. The difference in the depth of the lower cut-off of seismicity between different segments of the fault becomes less pronounced after single-event relocation using station corrections.

Acknowledgements

The authors acknowledge useful discussions with colleagues from DPRI, Kyoto University; ERI, University of Tokyo; NIED and University of Tsukuba. We thank Professor Yuji Yagi for useful suggestions to improve the manuscript. We are grateful to the Editor, Professor Katsuo Sashida, for his support and careful guidance.

References

Geospatial Information Authority of Japan (GSI), 1997. Crustal movements in the Chubu and Hokuriku districts, *Report of the Coordinating Committee for Earthquake Prediction*, **57**, 520-524, Tsukuba.

Geological Survey of Japan (GSJ), 2002. Geological map of Japan (CD-ROM), *Digital Geoscience*, **Map G-3**, 1:200000, Natl. Inst. of Adv. Ind. Sci. And Technol., Tsukuba, Japan.

Iio, Y., Sagiya, T., Kobayashi, Y., and Shiozaki, Y., 2002. Water-weakened lower crust and its role in the concentrated deformation in the Japanese Islands, *Earth and Planetary Science Letters*, **203**, 245-253.

Ito, K., 1990. Regional variations of cutoff-depth of seismicity in the crust and their relation to heat flow and large inland earthquakes, *Journal of Physics of* *the Earth*, **38**, 223-250.

Ito, K. and Wada, H., 2002. Observation of microearthquakes in the Atotsugawa fault region, central Honshu, Japan – Seismicity in the creeping section of the fault, in *Seismogenic Process Monitoring*, Edited by H. Ogasawara, T. Yanagidani and M. Ando, A.A. Balkema Publishers, Lisse, 229-243.

Ito, K., Wada, H., Ohmi, S., Hirano, N. and Ueno, T., 2007a. Seismic activity from routine and temporary observations of earthquakes in the northwest Chubu district, central Honshu, Japan, in *Geodynamics of Atotsugawa Fault System*, Edited by M. Ando, Terrapub, Tokyo, 45-63.

Ito, K., Ueno, T., Wada, H., and Matsumura, K., 2007b. Crustal structure from seismic surveys and seismicity in the northern Chubu district with special reference to the Atotsugawa fault area, in *Geodynamics of Atotsugawa Fault System*, Edited by M. Ando, Terrapub, Tokyo, 65-78.

Kato, A., Kurashimo, E., Hirata, N., Iwasaki, T., and Iidaka, T., 2006. Imaging crustal structure around the western segment of the Atotsugawa fault system, cental Japan, *Geophysical Research Letters*, **33**, L09307, doi:10.1029/2006GL025841.

Kato, A., Iidaka, T., Kurashimo, E., Nakagawa, S., Hirata, N., and Iwasaki, T., 2007. Delineation of probable asperities on the Atotsugawa fault, central Japan, using a dense temporary seismic network, *Geophysical Research Letters*, **34**, L09318, doi:10.1029/2007GL029604.

Kissling, E., Ellsworth, W.L., Eberhart-Phillips, D. and Kradolfer, U., 1994. Initial reference models in local earthquake tomography, *Journal of Geophysical Research*, **99**, 19635-19646.

Matsuda, T., 1966. Atotsugawa fault, *Bulletin of the Earthquake Research Institute, Tokyo University*, **44**, 1179-1212.

Mikumo, T., Wada, H., and Koizumi, M., 1988. Seismotectonics of the Hida region, central Honshu, Japan, *Tectonophysics*, **147**, 95-119.

Nakajima, J., and Hasegawa, A., 2007. Deep crustal structure along the Niigata-Kobe Tectonic Zone, Japan: its origin and segmentation, *Earth Planets Space*, **59**, e5-e8.

Nakajima, J., Kato, A., Iwasaki, T., Ohmi, S., Okada, T., Takeda, T., and "The Japanese University Group of the Joint Seismic Observations at NKTZ", 2010. Deep crustal structure around the Atotsugawa fault system, central Japan: A weak zone below the seismogenic zone and its role in earthquake generation, *Earth Planets Space*, **62**, 555-566.

Sagiya, T, S. Miyazaki and Tada, T., 2000. Continuous GPS array and present-day crustal deformation of Japan, *Pure and Applied Geophysics*, **157**, 2303-2322.

Shibutani, T., Iio, Y., Matsumoto, S., Katao, H., Matsushima, T., Ohmi, S., Takeuchi, F., Uehira, K., Nishigami, K., Enescu, B., Hirose, I., Kano, Y., Kohno, Y., Korenaga, M., Mamada, Y., Miyazawa, M., Tatsumi, K., Ueno, T., Wada, H., and Yukutake, Y., 2005. Aftershock distribution of the 2004 Mid Niigata Prefecture Earthquake derived from a combined analysis of temporary online observations and permanent observations, *Earth Planets Space*, **57**, 545-549.

Shimazaki, K., and Zhao, Y., 2000. Dislocation model for strain accumulation in a plate collision zone, *Earth Planets Space*, **52**, 1091-1094.

Sibson, R.H., 1982. Fault zone models, heat flow, and the depth distribution of earthquakes in the continental crust of the United States, *Bulletin of the Seismological Society of America*, **72**, 151-163.

The Japanese University Group of the Joint Seismic Observations at NKTZ, 2005. The Japanese university joint seismic observations at the Niigata-Kobe tectonic zone, *Bulletin of the Earthquake Research Institute, University of Tokyo*, **80**, 133–147 (in Japanese with English abstract).

The Research Group for Active Faults, 1991. *Active faults in Japan*, Univ. Tokyo Press, Tokyo.

Ueno, T., Ito, K., Yoshii, K., Matsumura, K., and Wada, H., 2005. Crustal structure and seismic activity around the Atotsugawa fault system, central Honshu, Japan, *Zisin*, 143–152.

Wada, H., and Ito, K., 1995. Seismic activity in the vicinity of the Atotsugawa fault, *Annuals of the Disaster Prevention Research Institute, Kyoto University*, **38**, 235-250 (in Japanese with English abstract).

Waldhauser, F., and Ellsworth, W.L., 2000. A double-difference earthquake location algorithm: method and application to the Northern Hayward Fault, California, *Bulletin of the Seismological Society of America*, **90**, 1353-1368.